Prediction of source contributions to surface PM$_{10}$ concentrations in European cities: a case study for an episode in December 2016 using EMEP/MSC-W rv4.15 - Part.2 The local urban background contribution

5   Matthieu Pommier[1,*]

1 Norwegian Meteorological Institute, Oslo, Norway
* now at Ricardo Energy and Environment, Harwell, Oxfordshire, UK.

10   Contact: matthieu.pommier@ricardo.com

Abstract.

Despite the progress made in the latest decades, air pollution is still the primary environmental cause of premature death in Europe. The urban population risks more likely to suffer to pollution related to high concentrations of air pollutants such as in

15   particulate matter smaller than 10 µm (PM$_{10}$). Since the composition of these particulates varies with space and time, the understanding of the origin is essential to determine the most efficient control strategies.

A source contribution calculation allows to provide such information and thus to determine the geographical location of the sources (e.g. city or country) responsible for the air pollution episodes. In this study, the calculations provided by the regional EMEP/MSC-W rv4.15 model in a forecast mode, with a 0.25° longitude × 0.125° latitude resolution, and based on a scenario

20   approach, have been explored. To do so, the work has focused on event occurring between 01 and 09 December 2016. This source contribution calculation aims at quantifying over 34 European cities the "Local" contribution of these PM$_{10}$, i.e. from the city itself, on an hourly basis. Since the methodology used in the model is based on reduced anthropogenic emissions, compared to a reference run, the choice of the percentage in the reductions has been tested by using three different values (5%, 15% and 50%). The definition of the "Local" contribution, and thus the definition of the area defining the cities is also an

25   important parameter. The impact of the definition of these urban areas, for the studied cities, was investigated (i.e. 1 model grid cell, 9 grid cells and the grid cells covering the definition given by the Global Administrative Area - GADM).

Using a 15% reduction in the emission and the use of larger cities for our source contribution calculation (e.g. 9 grid cells and GADM), help to reduce the non-linearity in the concentration changes. This non-linearity is observed in the mismatch between the total concentration and the sum of the concentrations from different calculated sources. When this non-linearity is observed,

30   it impacts the NO_3^-, NH_4^+ and H$_2$O concentrations. However, the mean non-linearity represents only less than 2% of the total modelled PM$_{10}$ calculated by the system.

During the studied episode, it was found that 20% of the predicted PM$_{10}$ had a "Local" origin, essentially composed of primary components. 60% of the hourly PM$_{10}$ concentrations predicted by the model came from the countries in the regional domain, and they were essentially composed of NO_3^-. The rest of the PM$_{10}$ was mainly due to natural sources. It was also shown that

35   the Central European cities were mainly impacted by the surrounding countries while the cities located a little away from the

rest of the other European countries (e.g. Oslo and Lisbon) had larger "Local" contribution. The usefulness of the forecasting

tool has also been illustrated with an example in Paris, since the system has been able to predict a local polluted event on 02

December 2016 as documented by local authorities.

40

45

50

55

60

65

Geoscientific
Model Development
Discussions

1. Introduction.

Air pollution is progressing up in the list of policy priorities for most the industrialized countries. However, even in Europe, progress still have to be made to reduce the levels of pollutant in the air. As shown by the European Environment Agency

70   (EEA), most people living in European cities are exposed to poor air quality (EEA report 2017). The European Court Auditors (ECA) also stipulates that air pollution is the biggest environmental risk to health in the European Union, with about 400 000 people who die each year prematurely due to excessive air pollutants (ECA, Special report 2018). They concluded that the European countries still not sufficiently protect their citizens' health. This shows that additional efforts need to be done at local and regional scales to improve the air quality.

75   One of this pollutant, the particulate matter smaller than 10 µm (PM_{10}), is related to premature mortality at high exposure. The World Health Organization (WHO) has established a short-term exposure PM_{10} guideline value of 50 µg/m³ daily mean that should not be exceeded in order to ensure healthy conditions (WHO, 2005). These PM_{10} can be emitted locally or transported on long distance. The origin of the PM_{10} can be anthropogenic such as the car traffic, the industry and the fuel combustion; and also natural such as the desert dust which can largely affect cities as Barcelona (e.g. Perez et al., 2012; Titos et al., 2017),

80   sea salt which has a large impact over the coastal cities (e.g. Hama et al., 2018) and emitted by the forest fires (e.g. Slezakova et al., 2013; Turquety et al., 2020). The PM_{10} are composed of primary components such as organic matter (OM), elemental carbon (EC), dust, sea salt, and other compounds. The PM_{10} are also composed of secondary components compounds formed by chemical reactions in the atmosphere from gas-phase precursors, such as nitrate (NO_3^-), ammonium (NH_4^+), sulphate (SO_4^{2-}), and a large range of secondary organic aerosol (SOA) compounds. These PM_{10} are essentially removed from the

85   atmosphere by wet deposition, even if dry deposition over different types of surface may have an important role. The variety of sources for these different components highlight the importance to estimate properly the source contributions in air quality modelling.

To provide information to identify the sources of the polluted events over different European cities, a forecasting source apportionment product has been developed within the Copernicus Atmosphere Monitoring Service (CAMS). The predictions

90   are calculated for 4 days and are available on the website https://policy.atmosphere.copernicus.eu/SourceContribution.php. The calculations are provided for the surface PM_{10} and its different components over European cities. The predictions are done as a complement to the country source contribution calculations, providing information on the countries responsible of the same polluted events. These country contributions are described in a companion paper (Pommier et al., 2020). The calculations, presented in this study, separate the "Local" contribution (i.e. city) from external contributions.

95   During the last decade, few methodologies have been applied to estimate the "Local" contribution to surface PM_{10} concentrations over the European cities through a modelling approach. For example, the SHERPA tool (Thunis et al., 2016), the TM5-FASST source-receptor model (Crippa et al.,2017) and the GAINS integrated assessment model (Kiesewetter et al., 2015), to cite a few, assume a linear relationship between concentration and emission changes. While the SHERPA tool bases

Geoscientific
Model Development
Discussions

100   its estimation on model scenarios from other regional models (EMEP/MSC-W model and CHIMERE), the GAINS model

combines past monitoring data with bottom-up emission modelling and a simplified atmospheric chemistry and dispersion

calculation. The TM5-FASST model is based on a set of emission perturbation experiments as done in our work. However,

the emission perturbation experiment, or also named the scenario approach, may cause non-linearity, i.e. the concentration

changes resulting from these perturbations over different sources are not necessarily equivalent to the sum of the individual

contribution from all these sources (e.g. Clappier et al., 2017). This shows that the impact of the non-linearity should be

105   analysed for the estimation of the source contribution.

None of the cited studies have provided daily or hourly predictions of "Local" contributions, whereas information is needed

to explain the origin of limit value exceedances in cities throughout Europe. Thus, the objective of this study is to present the

calculation of the "Local" contribution predicted by the EMEP/MSC-W model on hourly resolution. For the simplicity of the

reading, the EMEP/MSC-W model is hereafter referred to as EMEP model. This study has been focused on an event occurring

110   in Europe between the 01 and 09 December as described in Pommier al. (2020). This event was the first event listed from the

beginning of the development of system.

For the calculation of this "Local" contribution, the definition of the city area is a critical parameter. For this reason, the domain

defining the studied cities was investigated. To do so, 1 model grid cell ($0.25°$ longitude $\times$ $0.125°$ latitude), 9 grid cells and the

grid cells covering the definition given by the Global Administrative Area - GADM) have been used as also done in Pommier

115   al. (2020). The calculation of the "Local" contribution also depends on the concept used. Indeed, in this work the "Local"

contribution corresponds to the averaged concentration over a studied city. This uses a relatively coarse resolution, comparable

to the definition of the city domain used in previous studies such as in Thunis et al. (2016) who used an area of 35×35 km^2

or in Skyllakou et al. (2014) who used a radius of 50 km from the city center. In our definition of the "Local" contribution,

there is also no distinction between the urban background and the rural background which both may impact the concentration

120   of the pollutant over a city as explained in Thunis et al. (2018).

Section 2 provides a short introduction of the model set-up, i.e. a description of the model and of the experiment. Section 3

details the methodology used in the source contribution (SC) calculation. Section 4 explains the information calculated by the

SC during the episode. Section 5 describes the portion of the "Local" contribution over the European cities during the episode.

Finally, the conclusions are given in Section 6.

125   **2. The model set-up**

2.1. The EMEP model

The EMEP model is an Eulerian model described in detail in Simpson et al. (2012). Initially, the model has been aimed at

European simulations, but global scale modelling has been possible for many years (e.g. Wild et al., 2012) and applications

over other regions have already been done, such as in India (Pommier et al., 2018) and in China (Brasseur et al., 2019). The

130   EMEP model version rv4.15 has been used here in the forecast mode. The version rv4.15 has been described in Simpson et al.

(2017) and references cited therein. The main updates are explained in the companion paper (Pommier et al., 2020).

The chemical scheme couples the sulphur and nitrogen chemistry to the photochemistry using about 140 reactions between 70

species. The chemical mechanism is based on the "EMEP scheme" described in Simpson et al. (2012) and references therein.

The biogenic emissions of isoprene and monoterpene are calculated in the model by emission factors as a function of

135   temperature and solar radiation (Simpson et al., 2012).

In the EMEP model, PM emissions are split into EC, OM (here assumed inert) and the remainder, for both fine and coarse PM.

The OM emissions are further divided into fossil-fuel and wood-burning compounds for each source sector. As in Bergström

et al. (2012), the OM/OC ratios of emissions by mass are assumed to be 1.3 for fossil-fuel sources and 1.7 for wood-burning

sources. The model also calculates windblown dust emissions from soil erosion. Secondary aerosol consists of inorganic

140   sulphate, nitrate and ammonium, and SOA; the latter is generated from both anthropogenic and biogenic emissions, using the

'VBS' scheme detailed in Bergström et al (2012) and Simpson et al. (2012).

The main loss process for particles is wet-deposition, and the model calculates in-cloud and sub-cloud scavenging of gases

and particles as detailed in Simpson et al. (2012). Wet scavenging is treated with simple scavenging ratios, taking into account

in-cloud and sub-cloud processes.

145   In the EMEP model, the 3D precipitation is needed and an estimation of this 3D precipitation can be calculated by the model

if this parameter is missing in the meteorological fields. This estimate is derived from large scale precipitation and convective

precipitation. The height of the precipitation is derived from the cloud water. Then, it is defined as the highest altitude above

the lowest level, where the cloud water is larger than a threshold taken as 1.0×10^{-7} kg water per kg air. Precipitations are only

defined in areas where surface precipitations occur. The intensity of the precipitation is assumed constant over all heights

150   where they are non-zero

Gas and particle species are also removed from the atmosphere by dry deposition. This dry deposition parameterization follows

standard resistance-formulations, accounting for diffusion, impaction, interception, and sedimentation.

2.2. The experiment

The studied episode occurred from 01 to 09 December 2016 and the forecasts provided by the EMEP model cover Europe

155   (30°N-76°N, 30°W-45°E) (Pommier et al., 2020). An initial spin-up of 10 days was conducted. The model provides four-day

air quality forecasts, and the predicted fields have been used to initialise successive four-day forecasts. These predictions were

driven by forecasted meteorological fields at 12UTC from the previous day, with a 3-hour resolution, calculated by the

Integrated Forecasting System (IFS) of ECMWF. These forecasted meteorological fields correspond to the fields which were

used in the online production for these dates and used in the companion paper (Pommier et al., 2020). The ECMWF forecasts

160 do not include 3D precipitation, which is needed by the EMEP model as mentioned in Section 2.1. Therefore, a 3D precipitation

estimate is derived from IFS surface variables (large scale and convective precipitations).

The boundary conditions (BCs) at 00UTC of the current day from the atmospheric Composition module (C-IFS) have been

used. These BCs are specified for ozone (O_3), carbon monoxide (CO), nitrogen oxides (NO and NO_2), methane (CH_4), nitric

acid (HNO_3), peroxy-acetyl nitrate (PAN), SO_2, ISOP, ethane (C_2H_6), some VOCs, sea salt, Saharan dust and SO_4.

165 The TNO-MACC emission data set for 2011 on $0.25° \times 0.125°$ (longitude-latitude) resolution (Kuenen et al., 2014, see

http://drdsi.jrc.ec.europa.eu/dataset/tno-macc-iii-european-anthropogenic-emissions) has been used and the forest fire

emissions are from GFASv1.2 inventory (Kaiser et al., 2012).

Since this study aims quantifying the "Local" contribution from each city, the effect of the choice of the city domain has been

tested. The city edge has been defined by 1 grid cell (i.e. $0.25°$ lon $\times 0.125°$ lat, corresponding to the emissions data set

170 resolution), 9 grid cells and the all the grid cells covering the administrative area provided by the database of Global

Administrative Areas (GADM, https://gadm.org/data.html). This latter is the more precise definition in terms of buildup area,

however it may represent a large region as shown in Fig. 1a, such as Riga. It is also clear with Fig 1b that the 9 grid cells

domain corresponds to an extension of the 1 grid cell domain; and the area using the GADM definition may differ from the

two other definitions as over Ljubljana and in Switzerland.

175 The natural contributions are defined in this study as the sum of the contributions from sea salt, dust and forest fires.

3. Methodology of the EMEP source contribution calculation

3.1 Scenario approach: Emission reductions

The SC calculation follows the methodology uses in the country SC calculations (Pommier et al., 2020). The methodology is

a scenario approach and consists in estimating the concentration changes by performing and subtracting two simulations. In

180 our case, we have compared a reference run, where all the anthropogenic emissions are included, with a perturbation run,

where the emissions over a specific source are reduced. These perturbation runs which correspond to the simulations where

the emissions from every considered source region (e.g. a city) are reduced by 15%. As explained in Wind et al. (2004), a

reduction of 15% is sufficient to give a clear signal in the concentration changes. It also gives a negligible effect from non-

linearity in the chemistry. Moreover, it was shown that for the studied episode, the non-linearity, related to the emissions

185 reduction used, represented less than 2% of the total concentrations for each predicted country contribution (Pommier et al.,

2020). As performed in this companion study, the effect of the non-linearity, related to the percentage used in the perturbated

simulations, has been estimated in this work.

The perturbations are done for anthropogenic emissions of CO, SO_x, NO_x, NH_3, NMVOC and PPM (primary particulate

matter). For computational efficiency, all anthropogenic emissions in the perturbation runs have been reduced simultaneously.

190 It is worth noting that the non-linearity related to this simultaneous reduction in emissions have not been addressed in this

work for computational reason. Indeed, reducing the emissions simultaneously or separately may lead to a different result in the concentrations (e.g. Thunis et al., 2015).

The simulations correspond to perturbation runs over each capital of the 28 European Union capitals plus Barcelona, Bern, Oslo, Reykjavik, Rotterdam and Zurich. These simulations give the "Local" contribution for each city. For convenience, these city SC simulations were gathered by pair, such as Tallinn and Athens. It means that the pair of cities has their emissions reduced simultaneously. These pairs of cities have been chosen to do not impact on each other. In total, there are 17 pair runs. In addition, there is also a run where the external influence defined as "Rest of Europe" has been performed. This run presents reduced emissions over all the countries within the regional domain. Then, this "Rest of Europe" contribution has been calculated by the difference with the "Local" contribution. The calculated concentration of the pollutant integrated over the studied city, corresponds to the difference between the integrated concentration from the reference run and the integrated concentration of the perturbation run, scaled by 15%. The concentration is scaled by 15% since the concentration is assumed to be linear to the effect of a full contribution, i.e. a perturbation of 100%.

3.2 Limitation of the methodology: the chemical non-linearity

As explained previously, this methodology based on a scenario approach, may causes a non-linearity in the calculated concentrations. The total PM_{10} over the receptor should be theoretically identical to the sum of the PM_{10} originated from the different sources. This is not always the case and it might have few differences between the total PM_{10} and the sum from the various sources. To ensure the robustness of the methodology, as done in Pommier et al. (2020), the 15% perturbation has been tested and values of 5% and 50% in the perturbation runs were also used. By using these three different perturbations, the total number of simulations performed for this study is equal to 495 (17 pairs city × 9 dates × 3 perturbations+ 9 rest of EU × 3 perturbations + 9 reference runs). As mentioned earlier, the simultaneous reduction in emissions may also lead to the non-linearity in the concentrations, in response to the emission changes. This non-linearity has not been quantified for computational reason.

4. Information provided by the source contribution calculations during the episode

4.1 Origin of the PM_{10}

In December 2016, a PM episode was developed across North-Western Europe (Pommier et al., 2020). High concentrations were measured and predicted over Paris (Fig. 2); and on December 6th and 7th, concentrations at some measurement stations in France, Belgium, the Netherlands, Germany and Poland, exceeded the daily WHO limit value of 50 $\mu g/m^3$.

Figure 2 shows the "Local" contribution (city) but we have also estimated the "Rest of Europe" contribution, gathering the concentrations from all the European countries included in the regional domain. There are also the "Extra sources" which

220   gather essentially the natural sources (sea salt, forest fires and dust) and the BCs. The reader is invited to compare with the

Figure 1 in the companion paper, presenting the country contributors for the same time-series.

Figure 3 presents the mean composition for the "Local", "Rest of Europe and "Extra sources" PM_{10} contributions for all cities,

for all 4-d predictions (from 01-04 Dec to 09-12 Dec) and split into negative and positive concentrations. This figure shows

the composition of the different contributions and the effect of the chemical non-linearity. The positive concentrations show

225   the overall composition for each contribution, and the chemical reason of the non-linearity is revealed by the negative

contributions to the predicted PM_{10} concentrations (which it will be further explained in the next Section 4.2).

The figure shows the main contributors to the "Local" PM_{10} are the primary components, i.e. EC, POM and rest PPM (which

corresponds to the remainder of coarse and fine PPM) as showed by the positive concentrations (Fig. 3a). These three primary

components represent between 70% and 80% of the predicted "Local" PM_{10}. The value of the mean concentration depends on

230   the city definition and so on the average of the concentrations over different size of city (1 grid cell, 9 grid cells, GADM). The

mean PM_{10} concentration in a smaller area is larger, showing that with a smaller grid, the PM_{10} is less diffused over the

integrated area. The "Rest of Europe" PM_{10} is mainly influenced by NO_3^- (by ~35%) (Fig. 3b). This agrees with the result

given in the companion paper by the EMEP country SC, showing that the PM_{10} coming from 30 European countries have been

composed of 38% of NO_3^- (Pommier et al., 2020). The "30 European countries" in the country SC calculation corresponds to

235   the 30 European countries used in the study (27 EU countries + Iceland + Norway + Switzerland). The 31st country is the

"Domestic country", i.e. the country corresponding to the studied city (e.g. Spain for Barcelona).

Overall, 60% of the contributions to the surface PM_{10} calculated over the selected cities during this episode have been coming

from the "Rest of Europe", essentially NO_3^-, 20% have been "Local" from the primary components and another 20% have

been from the "Extra sources" mainly composed of natural sources (~60-70%). This general feature varies from city to city

240   and from date to date.

It shows that the main contributor of the PM_{10} during the episode was caused by the long-range transport. By combining the

information provided in Pommier et al. (2020), we can conclude, in average, the main contributor to the "Rest of Europe"

PM_{10} is mostly composed of the "Domestic country". In other words, that means this episode was mainly influenced by the

"Domestic" country and not by the cities.

245   **4.2 Impact of the non-linearity for each contribution**

In Figure 3, the non-linearity has been highlighted by the negligible negative contributions calculated for the "Local" and "Rest

of Europe" contributions and small negative contributions predicted in "Extra sources". As explained in Section 3.1., the non-

linearity and thus, these negative PM_{10} are a result of the assumed linearity in the chemistry to full reduction by using a

perturbation factor (5%, 15% or 50%). This impacts the NO_3^-, NH_4^+ and H_2O concentrations as shown in Fig. 3, which is a

250   consequence of gas-aerosol partitioning of the species.

These species are linked through chemical reactions. NH_3 may react with nitric acid (HNO_3) to form ammonium nitrate (NH_4NO_3). This is an equilibrium reaction, and thus the transition from solid to gaseous phase depend on relative humidity (e.g. Wang et al., 2020), explaining why the NO_3^-, NH_4^+ and H_2O concentrations are linked. In addition to this, the effect of the change in emissions depends on the atmospheric composition already present. This means that the results based on a

255   scenario approach as in our calculation will depend on the chemical regime. For example, an amount of NO_x emitted over a source can result in a certain NH_4NO_3 concentration in the city. If this NO_x is emitted in excess, i.e. within a NH_3 limited regime, a NO_x emission reduction will have a small effect at the receptor point. Thus, the combination of NO_x and NH_3 chemical regimes within different source regions may lead at the end to a mismatch between the sum of the contributions and the total PM_{10}, resulting to these negative concentrations. However, this non-linear effect only leads to negative concentrations

260   less than 0.2 $\mu g.m^{-3}$ (0.8%) of the mean PM_{10} concentrations.

The impact of the percentage used in the perturbation runs and the size of the city edges have no significant impact in the amount of negative "Extra sources" PM_{10} concentrations and it is very small on the "Local" and "Rest of Europe" concentrations (Fig. 3). As in the country SC, the use of larger grids reduces the amount of the negative PM_{10} concentrations and reduces globally the impact of the non-linearity. The 15% factor also reduces the negative non-linearity in the "Local"

265   concentrations (e.g. H_2O for the 9 grids and GADM runs).

Similarly to the methodology used in the country source apportionment (Pommier et al. 2020), we have compared the PM_{10} concentrations calculated by using the different percentages in the perturbation runs over the same city edges (Fig. 4). This gives an estimation of the impact of the non-linearity for each contribution. The non-linearity has been calculated for each hourly contribution (which can be positive or negative as shown in Fig. 3), as the standard deviation of the hourly contribution

270   obtained by the three reduced emissions scenarios, and weighted by the hourly mean of the total concentration by following the equation (1):

$$NONLIN_{Contrib} = \frac{\sqrt{\frac{\sum_{i=1}^{n}\left(Ccontrib_i - \overline{Ccontrib}\right)^2}{n}}}{Ctot} \times 100\% \qquad (1)$$

n corresponds to the number of perturbations used (n=3), Ccontrib is the hourly PM_{10} concentration for a specific contribution ("Local" or "Rest of Europe" or "Extra sources") and Ctot is the hourly PM_{10} concentration.

The mean non-linearity due to the "Local" contribution represents in maximum 0.3% of the total PM_{10}, and it represents in

275   maximum 1.7% from the "Rest of Europe" and the "Extra sources" as shown in Figure 4. It is worth noting the non-linearity from the "Extra sources" depends on the non-linearity from the two other contributions.

The limited impact of the non-linearity in the mean values shows that the responses to perturbation runs are robust. It is also important to note the non-linearity is slightly reduced by using the larger domains defining the cities (e.g. 9 grid cells), in a good agreement with the conclusions given by the country SC calculations (Pommier et al., 2020) and shown in Figure 3.

280 Figure 5 shows that this limited non-linearity impacts almost homogeneously all the cities in the "Local" contributions, as noted with the color scale, with small exception over Malta, Tallinn, Reykjavik and in Switzerland. The Central European cities (e.g. Berlin, Prague) are slightly more impacted by the non-linearity in the "Rest of Europe" and the "Extra sources" contributions. This is predictable due to the influence of the surrounding countries on their PM_{10} over the relatively large area defining the cities (at least $0.25°$ longitude $\times 0.125°$ latitude). The non-linearity also varies from date to date over the cities

285 (not shown). This non-linearity remains limited, since in maximum, 7% of all the calculated hourly external contributions (Rest of Europe or Extra sources) for all 4-day forecasts over the selected cities have a non-linearity higher than 5% (0.1% for the Local contribution – not shown).

5. Importance of the local contribution

5.1. Overview during the episode

290 Figure 6 shows the mean contribution of the "Local" PM_{10} on the total concentration for each city during this episode. To do so, we have calculated the mean ratio between the "Local" concentration and the total PM_{10} concentration for each date individually. Following the conclusions from Section 4, only the results related to a 15% reduction in the emissions and the city edges defined by 9 grids have been shown.

The surface background PM_{10} over the Central European cities were not mainly impacted by the "Local" sources which is

295 explained by the impact of the surrounding countries in these cities. This is also a good illustration of the statement given in Section 4 saying that the main contribution during the episode was from the "Rest of Europe", and essentially composed of "Domestic" (country) sources. At the opposite, cities such as Oslo and Lisbon, which did not experience large PM_{10} concentrations, had a local contribution close to 70% on December 02nd and 03rd and close to 65% on December 5th, respectively (Fig. 6). For Paris, where the larger peak is predicted on December 01st (Fig. 2), the "Local" contribution

300 represents 44% on this date. However, it is possible that this fraction of "local" PM_{10} is underestimated by the model. Indeed, in Pommier al. (2020), it has been shown that the regional model underestimates the larger hourly observed concentrations. This is predictable since a regional model, with a such resolution defining a city, mainly captures the urban background concentrations which is not necessarily represented by the measurements in urban stations.

5.2. Complementary information with the country source apportionment: comparison between two cities

305 As illustration of the episode, we have decided to focus on the two cities, Paris and London. The comparison between both cities in their PM_{10} concentrations highlights the possibility to use this source contribution calculations to understand the origin of the pollution. It may also help policy makers to identify a specific component which explains the concentration in PM_{10} for a particular day. Figure 7 shows the main country contributors and the "Local" contribution from 01 to 09 December 2016

predicted by the EMEP model over Paris while Figure 8 shows the results for London. The list of the country contributors are

310 related to the work done in Pommier et al. (2020) and correspond to the 28 EU members plus Iceland, Norway and Switzerland. The larger peaks in PM_{10} over Paris and London have been calculated for the December 01st and 02nd. These high concentrations over Paris mainly come from France with a large part coming from the city of Paris as predicted by the EMEP model (Fig. 7) while for the two first days over London, the PM_{10} mainly have a British origin, external to London (Fig. 8). It is also clear that London is more influenced by external sources and by natural sources than Paris during this period.

315 During the two first days over Paris, the "Local" contribution is attributed to primary components (rest PPM and EC, by 46% and 30% on Dec 01st and by 37% and 25% on Dec 2nd, respectively) as calculated by the EMEP model (not shown). This "Local" contribution is confirmed by the report from the Paris regional air observatory (see https://www.airparif.asso.fr/_pdf/publications/pollution-episode-paris-area_dec2016.pdf). Thus, Paris is a good illustration of the overall statement presented in Section 4.2. (Fig. 3a), concluding that the "Local" contribution during the episode over the

320 studied cities was dominated by the primary components. This domination of the primary components for this case also shows if policies to reduce the local emissions over this area were performed during the 02 December, the level of urban background PM_{10} would have been below the daily 50 ug/m^3 as recommended by WHO. For London, the EMEP model predicted that the British PM_{10} was mostly due to SO_4^{2-} (26%), showing that London has a different behavior than the overall statement presented by Fig. 3b, where the "Rest of Europe" contribution was mainly due to NO_3^-. The part of primary component on the British

325 PM_{10} is larger for the following days when the British contribution to PM_{10} is low.

6. Conclusions

This paper has presented the city source contribution product calculated by the EMEP model in a forecast mode and developed within the Copernicus Atmosphere Monitoring Service (CAMS). This product aims at identifying the sources responsible of the urban background PM_{10} concentrations and this work has focused on an event occurring from 01 to 09 December 2016

330 over Europe. While the companion paper (Pommier et al., 2020) presented an evaluation of the calculation for the country contributions over 34 European cities, this paper has described the complementary information given by the prediction of the "Local" contribution to the PM_{10} concentrations in the same cities.

During the studied episode, 20% of the predicted PM_{10} had "Local" origin, essentially composed of primary components, and 60% was from the countries in the regional domain (defined as "Rest of Europe"), essentially composed of NO_3^-. This country

335 contribution was mainly related to the Domestic country (e.g. Spain for Barcelona) (Pommier et al., 2020). The rest of the PM_{10} was mainly due to natural sources. It was also shown that the Central European cities were mainly impacted by the surrounding countries while the cities located a little apart from the rest of the other European countries (e.g. Oslo and Lisbon) had larger "Local" contribution.

340   The methodology used in the EMEP model to calculate the contributions, has been based on perturbated emissions, known as a scenario approach. Thus, the change in the reduced emissions has been tested by using three different percentages: 5%, 15% and 50%. The definition of the Local contribution, i.e. originating from the city itself and thus, the choice of the domain defining the edges of each studied city was also investigated. It was shown that the 15% reduction and the use of large city areas (9 grids or GADM) presented better results. The use of both parameters helps to prevent a larger impact of non-linearity in the chemistry, which is related to an assumed linear response in the concentrations due to changes in emissions. This non-

345   linearity impacts the NO_3^-, NH_4^+ and H_2O concentrations. It was shown this non-linearity has a modest impact on the Local contribution and essentially impacts the "Rest of Europe" contribution. For this contribution, the larger non-linearity (>5% of the total PM_{10}) represents only 7% of all the predicted hourly contributions over the different cities. This non-linearity has a slightly larger influence over the Central European cities for this "Rest of Europe" contribution, explained by the large impact of the surrounding countries, and thus from the different sources, on the urban PM_{10} in these cities. The non-linearity may

350   cause negative concentrations, but the negative contributions represented only less than 0.8% of the total concentrations.

The aim of the system is to predict in near-real time the local and external contributions to the surface background PM_{10} concentrations over different European cities, and it was shown the example of Paris has been a good illustration of the usefulness of the forecasting tool. The system has been able to predict a local polluted event occurring on 02 December 2016, as mentioned in a published report. It also confirms for this event that by reducing the emission of the local sources could help

355   to reach the level below the recommended daily threshold established by the WHO. However, the Local contribution presented in this work, over the studied cities, may be underestimated on hourly resolution as suggested in the companion paper (Pommier et al., 2020). In this companion paper, it was shown the regional model underestimates the largest hourly urban concentrations which is predictable due to the relatively coarse resolution used to define a city. An inter-comparison with another technique to estimate the local urban background concentrations, or with another model by applying the same scenario approach have

360   not been addressed in this work but it might be subject to another study by performing a full year evaluation.

365

370

Data availability

The EMEP model is an open source model available on https://doi.org/10.5281/zenodo.3355041. The data processing scripts are available on https://doi.org/10.5281/zenodo.4191038.

Author contribution

375   MP performed the experiment, analyzed the data and wrote the manuscript.

Competing interests

The author declares that there is no conflict of interest.

390

395

400

References

Bergström, R., Denier van der Gon, H. A. C., Prévôt, A. S. H., Yttri, K. E., and Simpson, D.: Modelling of organic aerosols over Europe (2002–2007) using a volatility basis set (VBS) framework: application of different assumptions regarding the formation of secondary organic aerosol, Atmos. Chem. Phys., 12, 8499-8527, https://doi.org/10.5194/acp-12-8499-2012,

405   2012.

Brasseur, G. P., Xie, Y., Petersen, A. K., Bouarar, I., Flemming, J., Gauss, M., Jiang, F., Kouznetsov, R., Kranenburg, R., Mijling, B., Peuch, V.-H., Pommier, M., Segers, A., Sofiev, M., Timmermans, R., van der A, R., Walters, S., Xu, J., and Zhou, G.: Ensemble forecasts of air quality in eastern China – Part 1: Model description and implementation of the MarcoPolo–

410   Panda prediction system, version 1, Geosci. Model Dev., 12, 33-67, https://doi.org/10.5194/gmd-12-33-2019, 2019.

Clappier, A., Belis, C. A., Pernigotti, D., and Thunis, P.: Source apportionment and sensitivity analysis: two methodologies with two different purposes, Geosci. Model Dev., 10, 4245-4256, https://doi.org/10.5194/gmd-10-4245-2017, 2017.

415   Crippa, M., Janssens-Maenhout, G., Guizzardi, D., Van Dingenen, R., and Dentener, F.: Sectorial and regional uncertainty analysis of the contribution of anthropogenic emissions to regional and global $PM_{2.5}$ health impacts, Atmos. Chem. Phys. Discuss., https://doi.org/10.5194/acp-2017-779, in review, 2017.

EEA Report No 13/2017, Air quality in Europe 2017, https://www.eea.europa.eu/publications/air-quality-in-europe-2017.

420

European Court Auditors, Special report no 23/2018: Air pollution: Our health still insufficiently protected (https://www.eca.europa.eu/Lists/ECADocuments/SR18_23/SR_AIR_QUALITY_EN.pdf

Hama, S. M. L., Cordell, R. L., Staelens, J., Mooibroek, D., Monks, P. S.: Chemical composition and source identification of

425   PM_{10} in five North Western European cities, 214, 135-149, Atmos. Res., https://doi.org/10.1016/j.atmosres.2018.07.014, 2018.

Kaiser, J. W., Heil, A., Andreae, M. O., Benedetti, A., Chubarova, N., Jones, L., Morcrette, J.-J., Razinger, M., Schultz, M. G., Suttie, M., and van der Werf, G. R.: Biomass burning emissions estimated with a global fire assimilation system based on observed fire radiative power, Biogeosciences, 9, 527-554, https://doi.org/10.5194/bg-9-527-2012, 2012.

430

Kuenen, J. J. P., Visschedijk, A. J. H., Jozwicka, M., and Denier van der Gon, H. A. C.: TNO-MACC_II emission inventory; a multi-year (2003–2009) consistent high-resolution European emission inventory for air quality modelling, Atmos. Chem. Phys., 14, 10963-10976, https://doi.org/10.5194/acp-14-10963-2014.

435   Kiesewetter, G., Borken-Kleefeld, J., Schöpp, W., Heyes, C., Thunis, P., Bessagnet, B., Terrenoire, E., Fagerli, H., Nyiri, A., and Amann, M.: Modelling street level PM_{10} concentrations across Europe: source apportionment and possible futures, Atmos. Chem. Phys., 15, 1539-1553, https://doi.org/10.5194/acp-15-1539-2015, 2015.

Perez, L., Tobías, A., Querol, X., Pey, J., Alastuey, A., Díaz, J., Sunyer, J.: Saharan dust, particulate matter and cause-specific

440   mortality: A case–crossover study in Barcelona (Spain), Env. Int., 48, 150-155, https://doi.org/10.1016/j.envint.2012.07.001, 2012.

Pey, J., Querol, X., Alastuey, A.: Discriminating the regional and urban contributions in the North-Western Mediterranean: PM levels and composition Atmos. Env., 44, 1587-1596, doi:10.1016/j.atmosenv.2010.02.005, 2010.

445

Pommier, M., Fagerli, H., Gauss, M., Simpson, D., Sharma, S., Sinha, V., Ghude, S. D., Landgren, O., Nyiri, A., and Wind, P.: Impact of regional climate change and future emission scenarios on surface O_3 and $PM_{2.5}$ over India, Atmos. Chem. Phys., 18, 103-127, https://doi.org/10.5194/acp-18-103-2018, 2018.

450   Pommier, M., Fagerli, H., Schulz, M., Valdebenito, A., Kranenburg, R., and Schaap, M.: Prediction of source contributions to urban background PM_{10} concentrations in European cities: a case study for an episode in December 2016 using EMEP/MSC-W rv4.15 and LOTOS-EUROS v2.0 – Part 1: The country contributions, Geosci. Model Dev., 13, 1787–1807, https://doi.org/10.5194/gmd-13-1787-2020, 2020.

455   Simpson, D., Benedictow, A., Berge, H., Bergström, R., Emberson, L. D., Fagerli, H., Flechard, C. R., Hayman, G. D., Gauss, M., Jonson, J. E., Jenkin, M. E., Nyíri, A., Richter, C., Semeena, V. S., Tsyro, S., Tuovinen, J.-P., Valdebenito, Á., and Wind, P.: The EMEP MSC-W chemical transport model – technical description, Atmos. Chem. Phys., 12, 7825-7865, https://doi.org/10.5194/acp-12-7825-2012, 2012.

460   Simpson, D., Bergström, R., Imhof, H., and Wind, P.: Updates to the EMEP/MSC-W model, 2016-2017 Transboundary particulate matter, photo-oxidants, acidifying and eutrophying components. EMEP Status Report 1/2017, The Norwegian Meteorological Institute, Oslo, Norway, 15-36, ISSN 1504-6109, 2017.

Skyllakou, K., Murphy, B. N., Megaritis, A. G., Fountoukis, C., and Pandis, S. N.: Contributions of local and regional sources

465   to fine PM in the megacity of Paris, Atmos. Chem. Phys., 14, 2343-2352, https://doi.org/10.5194/acp-14-2343-2014, 2014.

Slezakova K., Morais, S., do CarmoPereira, M.: Forest fires in Northern region of Portugal: Impact on PM levels, Atmos.

Res., 148-153, https://doi.org/10.1016/j.atmosres.2012.07.012, 2013.

470   Titos, G., Ealo, M., Pandolfi, M., Pérez, N., Sola, Y., Sicard, M., Comerón, A., Querol, X., and Alastuey, A. : Spatiotemporal

evolution of a severe winter dust event in the western Mediterranean: Aerosol optical and physical properties,J. Geophys. Res.

Atmos., 122, 4052–4069, doi:10.1002/2016JD026252, 2017.

Thunis, P., Clappier, A., Pisoni, E., Degraeuwe, B.: Quantification of non-linearities as a function of time averaging in regional

475   air quality modeling applications, Atmos. Env., 103, 263-275, https://doi.org/10.1016/j.atmosenv.2014.12.057, 2015.

Thunis, P., Degraeuwe, B.,Pisoni, E., Ferrari, F., Clappier, A.: On the design and assessment of regional air quality plans: The

SHERPA approach, Journal of Env. Management, 183, 952-958, https://doi.org/10.1016/j.jenvman.2016.09.049, 2016.

480   Thunis, P., Degraeuwe, B., Pisoni, E., Trombetti, M., Peduzzi, E., Belis, C. A., Wilson, J., Clappier, A., Vignati, E.: $PM_{2.5}$

source   allocation   in   European   cities: A   SHERPA   modelling   study,   Atmos.   Env.,   187,   93-106,

doi.org/10.1016/j.atmosenv.2018.05.062, 2018.

Turquety, S., Menut, L., Siour, G., Mailler, S., Hadji-Lazaro, J., George, M., Clerbaux, C., Hurtmans, D., and Coheur, P.-F.:

485   APIFLAME v2.0 biomass burning emissions model: impact of refined input parameters on atmospheric concentration in

Portugal in summer 2016, Geosci. Model Dev., 13, 2981–3009, https://doi.org/10.5194/gmd-13-2981-2020, 2020.

Wang, M., Kong, W., Marten, R. et al.: Rapid growth of new atmospheric particles by nitric acid and ammonia condensation.

Nature 581, 184–189, https://doi.org/10.1038/s41586-020-2270-4, 2020.

490

WHO Air quality guidelines for particulate matter, ozone, nitrogen dioxide and sulfur dioxide - Global update 2005 - Summary

of   risk   assessment   (available   on

https://apps.who.int/iris/bitstream/handle/10665/69477/WHO_SDE_PHE_OEH_06.02_eng.pdf?sequence=1).

495   Wild, O., Fiore, A. M., Shindell, D. T., Doherty, R. M., Collins, W. J., Dentener, F. J., Schultz, M. G., Gong, S., MacKenzie,

I. A., Zeng, G., Hess, P., Duncan, B. N., Bergmann, D. J., Szopa, S., Jonson, J. E., Keating, T. J., and Zuber, A.: Modelling

future changes in surface ozone: a parameterized approach, Atmos. Chem. Phys., 12, 2037-2054, https://doi.org/10.5194/acp-

12-2037-2012, 2012.

500   Wind, P., Simpson, D., Tarrasón, L.: Chap. 4 Source-receptor calculations, EMEP Status Report 1/2004: "Transboundary

acidification, eutrophication and ground level ozone in Europe", Joint MSC-W & CCC & CIAM & ICP-M&M & CCE Report,

ISSN 0806-4520, 2004.

505

510

515

520

525

a)
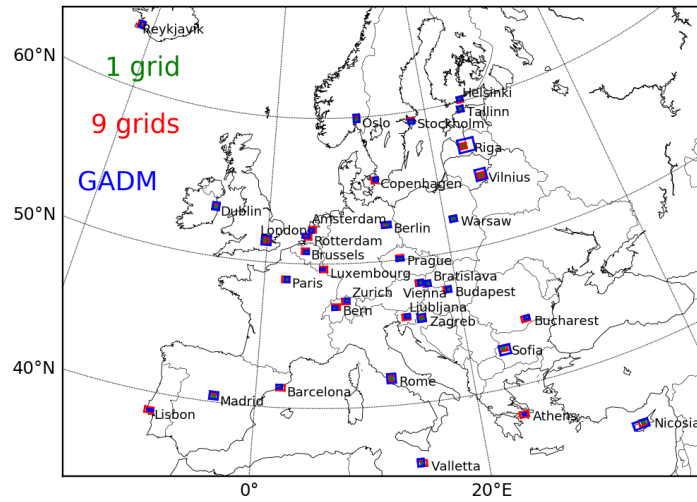
b)
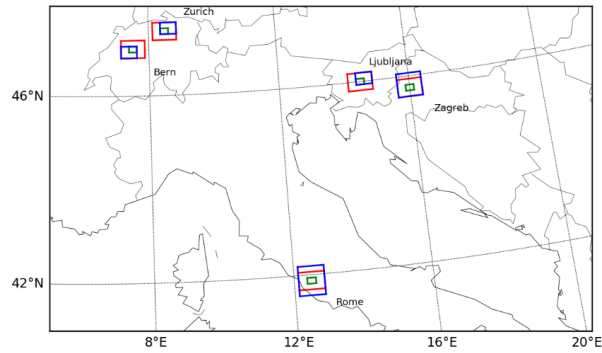
Figure 1: a: Boxes defining each city edge, based on the 1 grid (green), 9 grids (red) and the GADM (blue) definitions, b: Zoom on a few cities highlighting the difference between the three definitions.
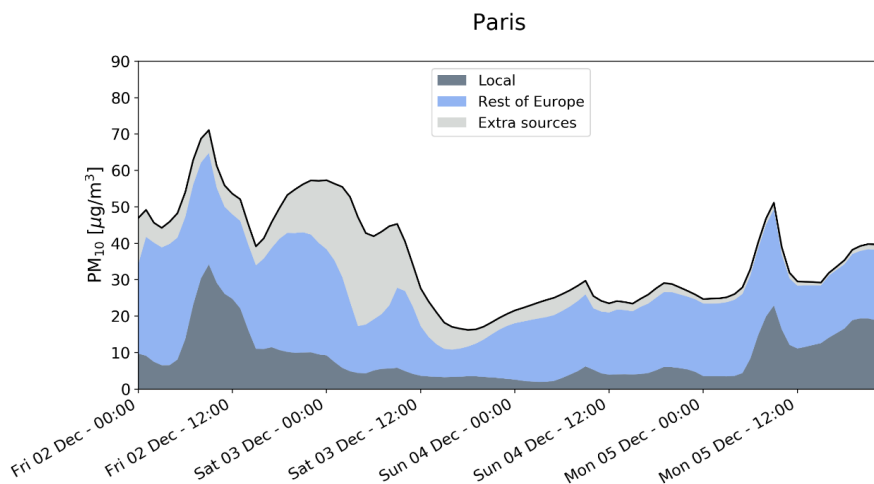
Figure 2: Hourly PM$_{10}$ concentrations in µg/m^3 predicted by the EMEP model over Paris (defined by 9 grid cells) from 02 December to 05 December 2016. The black curve highlights the total concentration. The "local", "Rest of Europe" and "Extra sources" contributions are provided. "Local" corresponds to the city contribution. "Rest of Europe" corresponds to all the European countries included in the regional domain and excluding the "Local" contribution. "Extra sources" include the natural sources, the boundary conditions, the ship traffic, the biogenic sources, the soil NO emission, the aircraft emission and the lightning.

530

535

540
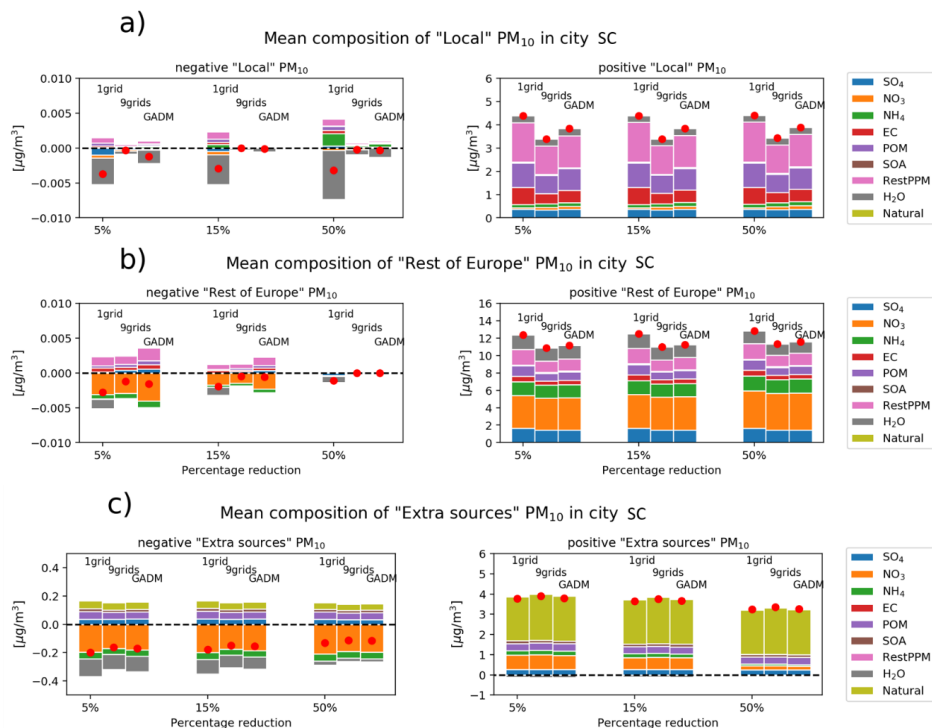
Figure 3: Mean composition of "Local" (a), "Rest of Europe" (b), and "Extra sources" PM$_{10}$ split into a negative concentration (left panel) and a positive concentration (right panel), calculated by the EMEP city source contribution over the 34 European cities and for each 4day-forecast. The PM$_{10}$ composition is highlighted with the color code. The results for the 3 city definitions (1 grid cell, 9 grid cells, GADM) and for the percentage of reduction used in the perturbation runs (5%, 15%, 50%) are shown. The "Local" contribution corresponds to the contribution from the city. "Rest of Europe" corresponds to all the European countries included in the regional domain and excluding the "Local" contribution. "Extra sources" include the natural sources, the boundary conditions, the ship traffic, the biogenic sources, the soil NO emission, the aircraft emission and the lightning. The red dot represents the mean PM$_{10}$ concentration.
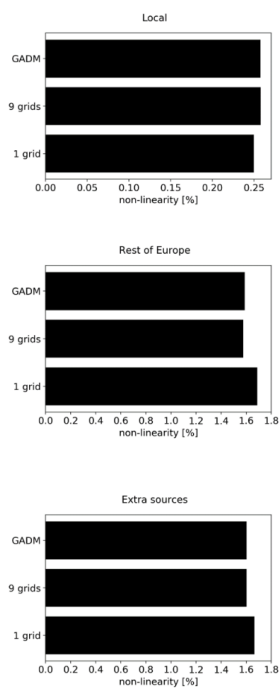
Figure 4: The black horizontal bars show the mean non-linearity calculated for each contribution presented in Figure 3 and for the three city definitions. The non-linearity is calculated for each hourly concentration as the standard deviation of the hourly contribution weighted by the hourly mean of the total concentration.
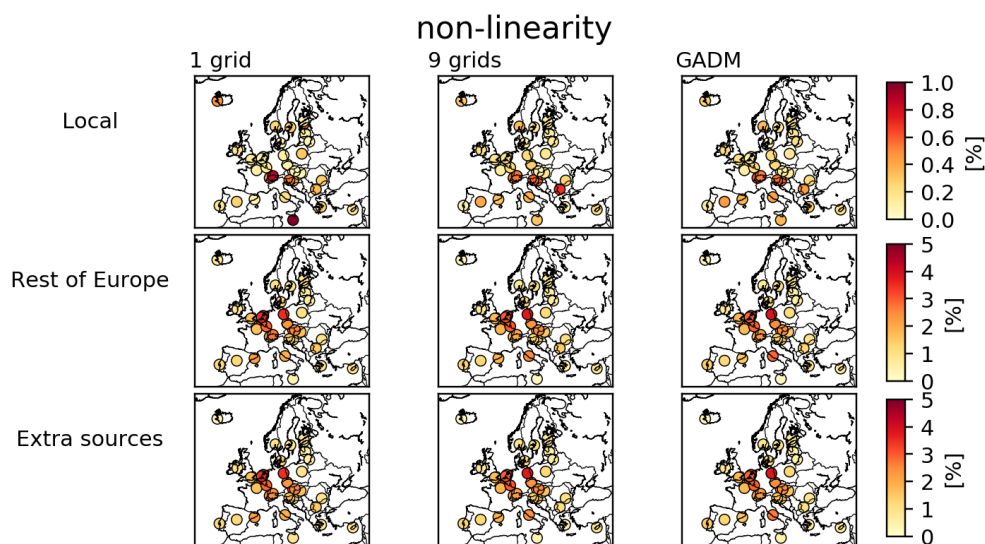

Figure 5: Mean non-linearity in percent calculated for the "Local", "Rest of Europe" and "Extra sources" contributions, over the 34 European cities and for each 4day-forecast (i.e. from 01-04 Dec to 09-12 Dec 2016). The non-linearity is presented for the cities defined by 1 grid (left row), 9 grids (middle row) and by the GADM (right row). Note the different scale to the "Local" contribution compared to the two others.
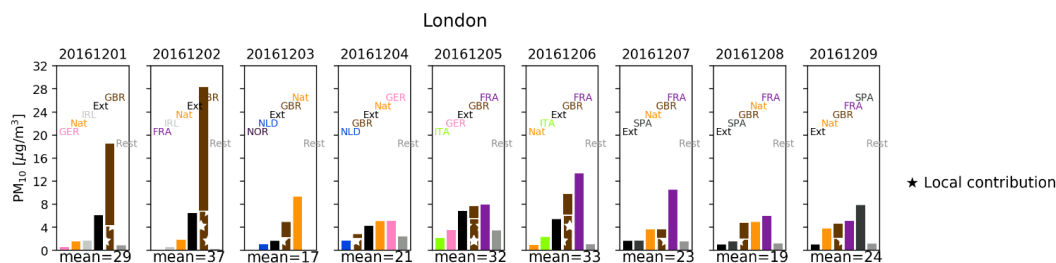
21
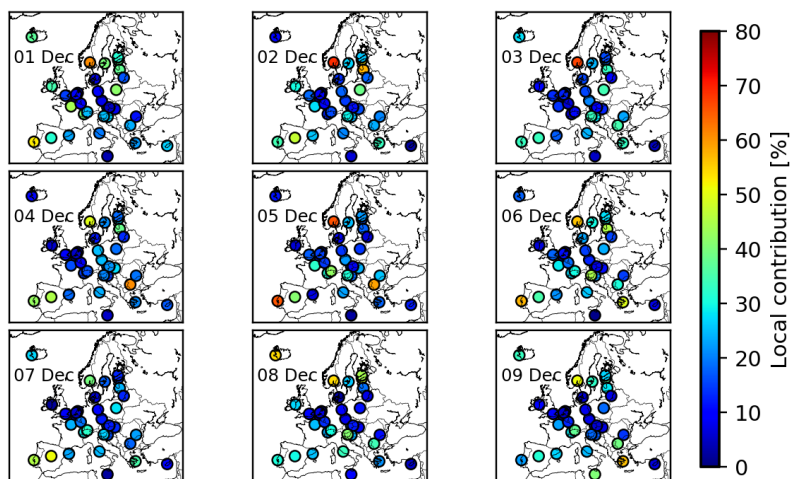
9 grids - EMEP pertubation factor: 15%

Figure 6: Mean Local contribution for each city from 01 to 09 December 2016. Each city edge is defined by 9 grid cells. The contribution is based on the calculations performed by the 15% perturbation runs.
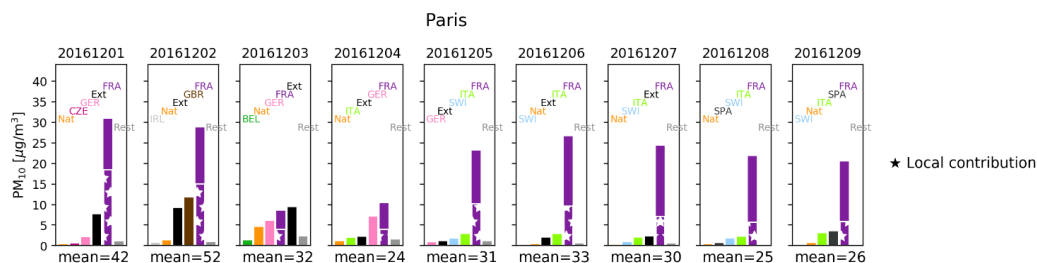
Figure 7: Main country contributors to surface PM$_{10}$ over Paris, defined by 9 grid cells, for each single day from 01 to 09 December 2016 predicted by the EMEP model (see Pommier et al., 2020). The five main contributors are plotted as well as the difference between the daily mean and the sum of these five contributors ("Rest"). The "external" contributor ("Ext" on the figure) essentially corresponds to the countries not included in the country SC runs and the BCs. The "Local" contribution is highlighted by white stars. The daily mean surface PM$_{10}$ concentration is written below each bar chart.

Figure 8: As Fig. 7 for London.